

# Use of nanoparticles to monitor human mesenchymal stem cells transplanted into penile cavernosum of rats with erectile dysfunction

Jae Heon Kim, Hong Jun Lee<sup>1</sup>, Seung Hwan Doo, Won Jae Yang, Dongho Choi<sup>2</sup>, Jung Hoon Kim<sup>3</sup>, Jong Ho Won<sup>4</sup>, Yun Seob Song

Department of Urology, Soonchunhyang University Seoul Hospital, Soonchunhyang University College of Medicine, Seoul, <sup>1</sup>Medical Research Institute, Chung-Ang University College of Medicine, Seoul, <sup>2</sup>Department of Surgery, Hanyang University School of Medicine, Seoul, <sup>3</sup>Department of Radiology, Seoul National University College of Medicine, Seoul, <sup>4</sup>Department of Oncology and Hematology, Soonchunhyang University Seoul Hospital, Soonchunhyang University College of Medicine, Seoul, Korea

**Purpose:** This study was performed to examine the treatment of erectile dysfunction by use of superparamagnetic iron oxide nanoparticles-labeled human mesenchymal stem cells (SPION-MSCs) transplanted into the cavernous nerve injured cavernosa of rats as monitored by molecular magnetic resonance imaging (MRI).

**Materials and Methods:** Eight-week-old male Sprague-Dawley rats were divided into three groups of 10 rats each: group 1, sham operation; group 2, cavernous nerve injury; group 3, SPION-MSC treatment after cavernous nerve injury. Immediately after the cavernous nerve injury in group 3, SPION-MSCs were injected into the cavernous nerve injured cavernosa. Serial T2-weighted MRI was done immediately after injection and at 2 and 4 weeks. Erectile response was assessed by cavernous nerve stimulation at 2 and 4 weeks.

**Results:** Prussian blue staining of SPION-MSCs revealed abundant uptake of SPION in the cytoplasm. After injection of  $1 \times 10^6$  SPION-MSCs into the cavernosa of rats, T2-weighted MRI showed a clear hypointense signal induced by the injection. The presence of SPION in the corpora cavernosa was confirmed with Prussian blue staining. At 2 and 4 weeks, rats with cavernous nerve injury had significantly lower erectile function than did rats without cavernous nerve injury ( $p < 0.05$ ). The group transplanted with SPION-MSCs showed higher erectile function than did the group without SPION-MSCs ( $p < 0.05$ ). The presence of SPION-MSCs for up to 4 weeks was confirmed by MRI imaging and Prussian blue staining in the corpus cavernosa.

**Conclusions:** Transplanted SPION-MSCs existed for up to 4 weeks in the cavernous nerve injured cavernosa of rats. Erectile dysfunction recovered and could be monitored by MRI.

**Keywords:** Erectile dysfunction; Magnetic resonance imaging; Mesenchymal stem cell transplantation; Nanoparticles

---

This is an Open Access article distributed under the terms of the Creative Commons Attribution Non-Commercial License (<http://creativecommons.org/licenses/by-nc/3.0>) which permits unrestricted non-commercial use, distribution, and reproduction in any medium, provided the original work is properly cited.

---

**Received:** 23 December, 2014 • **Accepted:** 27 January, 2015

**Corresponding Author:** Yun Seob Song

Department of Urology, Soonchunhyang University Seoul Hospital, Soonchunhyang University College of Medicine,  
59 Daesagwan-ro, Yongsan-gu, Seoul 140-743, Korea  
TEL: +82-2-709-9375, FAX: +82-2-709-9378, E-mail: yssong@schmc.ac.kr

© The Korean Urological Association, 2015

[www.kjuurology.org](http://www.kjuurology.org)

## INTRODUCTION

Radical prostatectomy is a widely used treatment for clinically localized prostate cancer. Yet, even with the advent of the nerve-sparing approach, erectile dysfunction (ED) remains a major complication of the procedure [1]. Although phosphodiesterase type 5 inhibitor therapy is a commonly used first-line treatment for ED following bilateral nerve-sparing radical prostatectomy, these drugs remain largely inefficient in this population [2,3].

Recently, stem cell-based therapy has garnered attention as a potential alternative in the prevention of ED following cavernous nerve (CN) injury. Adult bone marrow-derived stem cells can preserve erectile function via intracavernous application [4,5]. However, despite the apparent therapeutic efficacy of stem cell transplantation, *in vivo* monitoring of this approach has rarely been investigated. This information is important before future human clinical trials can be initiated. Reliable *in vivo* monitoring of transplanted cells will enable a systematic investigation of cell therapy.

Most *in vivo* monitoring of transplanted cells has historically utilized immunohistochemical staining, which requires the sacrifice of the experimental animals. By using molecular imaging with nanoparticles, the biological processes of the transplanted stem cells can be monitored noninvasively, and monitoring can be possible in the same host [6,7]. Moreover, serial consecutive monitoring can be achieved with the aid of magnetic resonance imaging (MRI) or optical imaging including positron emission tomography and single-photon emission computed tomography.

Molecular imaging techniques that include optical imaging and MRI provide high resolution and sensitivity for transplanted cells [8]. Superparamagnetic iron oxide nanoparticles (SPION) are being used for intracellular magnetic labeling of stem cells in the urologic field [9,10]; the nanoparticles reduce the T2 relaxation time and facilitate MRI detection of labeled cells.

The present study monitored the fate of human mesenchymal stem cells (MSCs) after intracavernous injection following CN injury and evaluated the resulting improvement of ED.

## MATERIALS AND METHODS

### 1. Harvest and culture of human MSCs

Human MSCs were harvested and cultured as reported previously [9-11]. Bone marrow was harvested by puncture aspiration of 10 to 20 mL by use of a sterile technique from the posterior iliac crest. Bone marrow transplantation was

done after informed consent from the donors. Isolation of mononuclear cells was done by Ficoll-Hypaque (Sigma-Aldrich, St Louis, MO, USA) density centrifugation. After collection and washing of mononuclear cells, the cells were resuspended to a final density of  $2 \times 10^5/\text{cm}^2$ . The cells were cultured in Dulbecco's modified Eagle's medium with low glucose (DMEM-LG, GibcoBRL, Grand Island, NY, USA) including 10% fetal bovine serum (GibcoBRL) and 1% antibiotic-antimycotic solution (GibcoBRL). The cells were placed in 75-cm<sup>2</sup> flasks (Falcon, Franklin Lakes, NJ, USA) and were incubated at 37°C and 5% CO<sub>2</sub> with 95% relative humidity. The medium was exchanged after 72 hours and then every 3 to 4 days thereafter. When the cultures reached approximately 90% confluence, MSCs were detached with 0.05% trypsin-ethylenediaminetetraacetic acid solution (GibcoBRL). Cells were then replaced for passage culture at a density of  $1 \times 10^6$  cells per 175-cm<sup>2</sup> flask. In the final cultured MSCs, negative hematopoietic markers were confirmed by flow cytometry and the ability of the cells to differentiate into osteocytes, chondrocytes, and adipocytes *in vitro* was verified [9].

### 2. Iron oxide particle labeling

As described previously [9,10], the liposome transfection agent GenePORTER (GTS, San Diego, CA, USA) was used for *in vitro* MRI analysis of SPION-labeled MSCs. A stock solution of GenePORTER was mixed into the culture medium at a dilution of 1:250, which was again mixed with SPION (Feridex, AMI, Cambridge, MA, USA) for 60 minutes at room temperature. Labeled cells were harvested by gene trypsinization for transplantation. The efficiency of the labeling of the SPION-MSCs was checked with Prussian blue staining and electron microscopy (H-7600, Hitachi, Tokyo, Japan). Cell viability was assessed with Trypan blue staining.

### 3. *In vivo* MRI

MRI examinations of the back muscle of rats were performed with T2-weighted images after transplantation of SPION-MSCs [9,10] with adjustment for the various concentrations of SPION-MSCs used. Consecutive serial T2-weighted MRI was performed for up to 4 weeks.

### 4. Transplantation of human MSCs into rat penile cavernosum

Three groups of 10-week-old male Sprague Dawley rats (300–320 g, n=30) were used in this study under approval of the Soonchunhyang Institutional Animal Care Committee. MSCs were transplanted into rat penile cavernosum as

described previously [9,10]. Group 1 (n=10) was the sham-operated group. Group 2 (n=10) was the CN injury group without SPION-MSCs transplantation. Group 3 (n=10) was the CN injury group with transplantation of SPION-MSCs. Anesthesia was done with 1% ketamine (30 mg/kg) and xylazine hydrochloride (4 mg/kg). During the operation, the cavernosal nerve and major pelvic ganglion were exposed around the prostate. In the sham group no further procedure was done, whereas in groups 2 and 3, the cavernosal nerve was identified and mechanical crushing injury was performed on both sides with a hemostat. Then the penile skin was incised and the cavernosum was identified and palpated. SPION-MSCs ( $1 \times 10^6$ ) were injected into the cavernosum by using a 500- $\mu$ L syringe with a 26-gauge needle. Before transplantation, an elastic tourniquet was placed at the penile base for 2 minutes. The penile cavernosal tissue was obtained at 2 and 4 weeks after SPION-MSCs transplantation.

### 5. *In vivo* measurement of erectile function

Intracavernous pressure (ICP) was measured at 2 and 4 weeks after the operation as described previously [9,10]. *In vivo* measurement of ICP was done under anesthesia with intraperitoneal injection of 1% ketamine (30 mg/kg) and xylazine hydrochloride (4 mg/kg). After the major pelvic ganglion and CN around the prostate were exposed, an electrical probe was placed at the CN. ICP was measured after stimulation of the CN with 1 V at a frequency of 12 Hz and square-wave duration of 1 ms for 1 minute. Mean arterial pressure (MAP) was measured at the carotid artery

after dissecting the neck to control the variance in systolic blood pressure. The measured parameters were ICP, maximal ICP, and ratio of maximal ICP/MAP.

### 6. Histological examination

After the last serial *in vivo* MRI, the rats were anesthetized again and killed by injection of cold saline directly into the heart. Penile tissue was harvested and fixed with 4% paraformaldehyde, and then the penis was cryoprotected and sectioned by use of a CM 1900 cryostat (Leica, Solms, Germany). Finally, the specimens were stained with hematoxylin and eosin or Prussian blue.

### 7. Statistical analysis

One-way analysis of variance and the *post hoc* Turkey test were used for analysis. Data are presented as mean  $\pm$  standard deviation. A p-value less than 0.05 was considered statistically significant.

## RESULTS

### 1. Cell labeling and histological analysis

Human MSCs were separated and SPION were transfected into MSCs *in vitro* by use of the GenePORTER transfection agent. Prussian blue staining of labeled MSCs revealed abundant uptake of the SPION-GenePORTER complex in the cytoplasm. However, no stainable iron was detected in the unlabeled MSCs (Fig. 1).

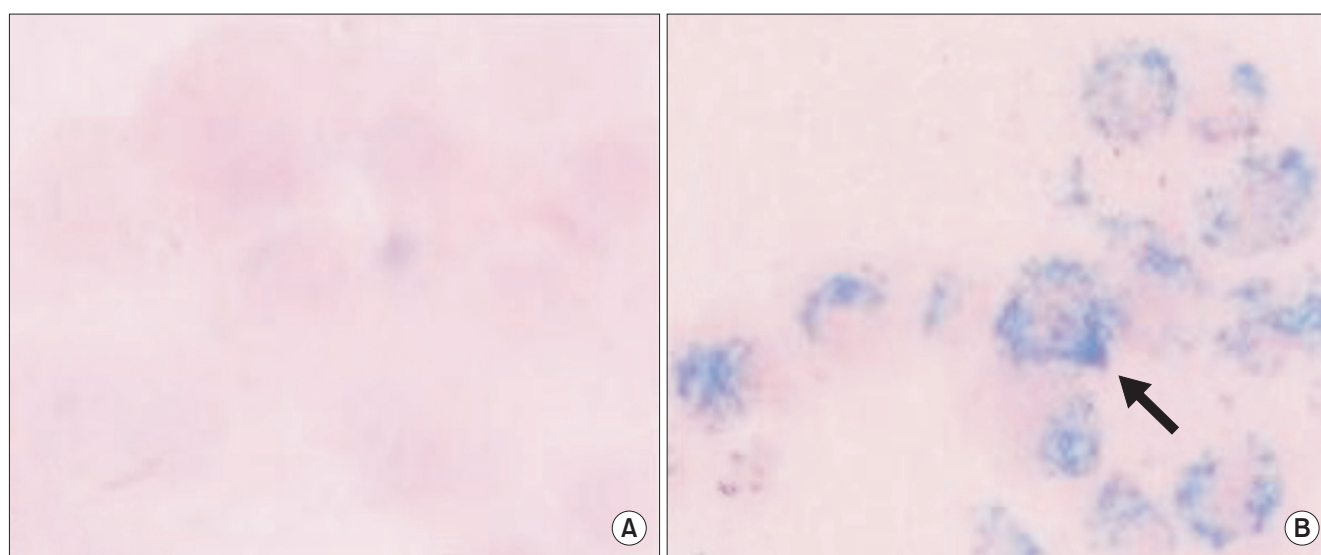


**Fig. 1.** Prussian blue staining of human mesenchymal stem cells with or without superparamagnetic iron oxide nanoparticles labeling. (A) Prussian blue-stained unlabeled human mesenchymal stem cells ( $\times 400$ ). (B) Prussian blue-stained labeled human mesenchymal stem cells ( $\times 400$ ). Note the abundant iron particles (blue dots) in the cytoplasm of the cells (arrow).

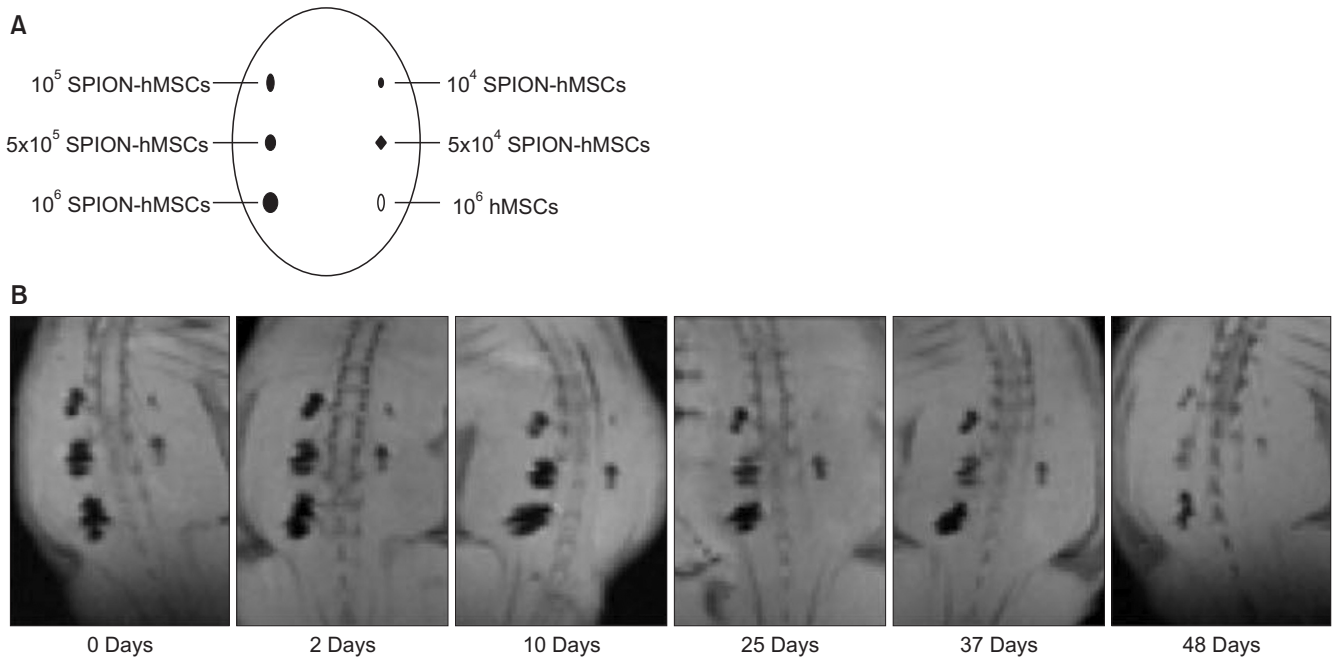


**Fig. 2.** (A) Schematic view of *in vivo* MRI according to the concentration of SPION-labeled hMSCs on the back muscle of rats (10<sup>5</sup> SPION-hMSCs, 5x10<sup>5</sup> SPION-hMSCs, 10<sup>6</sup> SPION-hMSCs, 10<sup>4</sup> SPION-hMSCs, 5x10<sup>4</sup> SPION-hMSCs, 10<sup>6</sup> hMSCs/mL). MRI showed a clear hypointense signal at all concentrations greater than 1x10<sup>5</sup> SPION-hMSCs/mL. (B) *In vivo* MR image according to the duration SPION-labeled human MSCs on the back muscle of rats. MRI showed a clear hypointense signal until 48 days after transplantation. MRI, magnetic resonance imaging; SPION, superparamagnetic iron oxide nanoparticles; hMSCs, human mesenchymal stem cells.

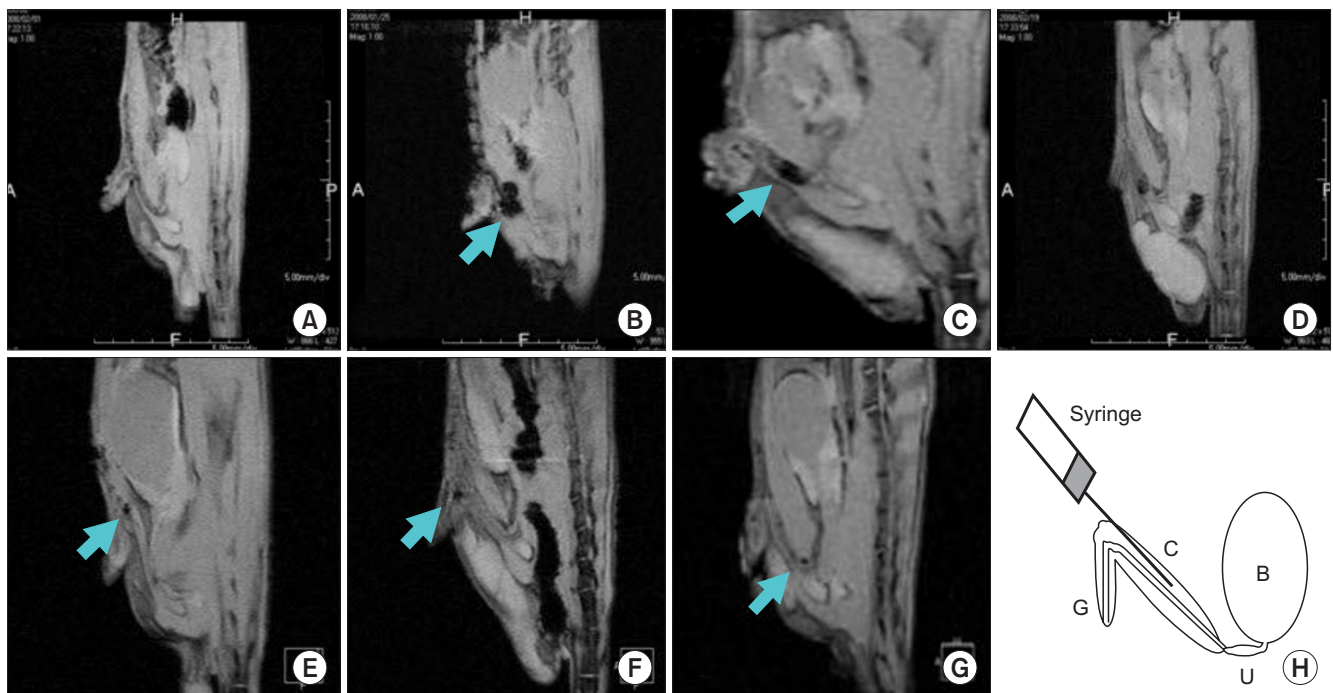


**Fig. 3.** *In vivo* MRI of magnetically labeled hMSCs. (A) Before transplantation in rat. (B) Immediately after transplantation in rat. (C) At 1 week after transplantation in rat. (D) At 2 weeks after transplantation in rat. (E) At 4 weeks after transplantation in rat. (F) At 6 weeks after transplantation in rat. (G) At 12 weeks after transplantation in rat. (H) Schematic drawing of glans penis, cavernosum, urethra, bladder, and transplanted hMSCs. Arrow shows the decrease of MR signal intensity. The areas of decreased MR signal intensity in the in the penile cavernosum were confined locally. G, glans penis; C, cavernosum; U, urethra; B, bladder; MRI, magnetic resonance imaging; hMSCs human mesenchymal stem cells.

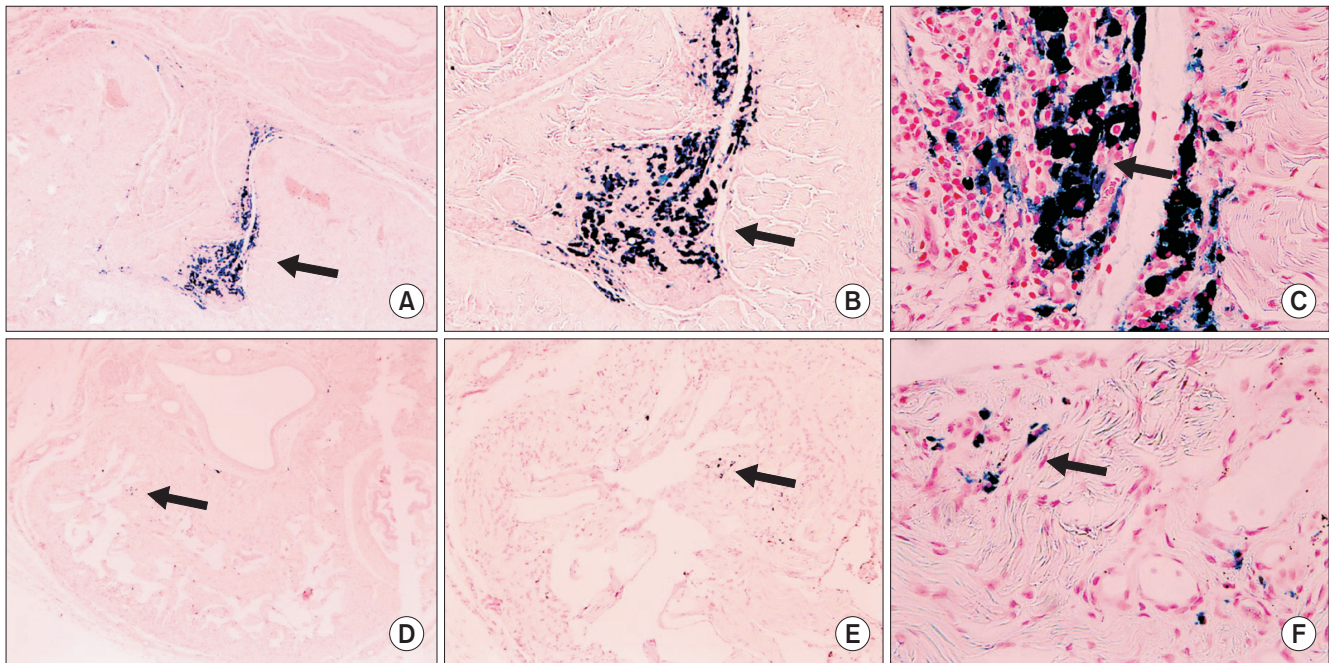


**Fig. 4.** Histologic findings of magnetically labeled human mesenchymal stem cells in rat corpus cavernosum after transplantation by use of Prussian blue staining. (A–C) Two weeks after transplantation (A:  $\times 40$ ; B:  $\times 100$ ; C:  $\times 400$ ). (D–F) Four weeks after transplantation (D:  $\times 40$ ; E:  $\times 100$ ; F:  $\times 400$ ). Intracytoplasmic SPION particles (blue dots) are clearly visible with Prussian blue staining (arrows). SPION, superparamagnetic iron oxide nanoparticles.

## 2. Viability

SPION-MSCs were cultured for 6 days and the viability of the labeled cells was measured by using Trypan blue staining. The viabilities of MSCs with and without SPION-labeling were 98% and 95%, respectively.

## 3. *In vivo* MRI

*In vivo* MRI according to the concentration of SPION-MSCs showed a clear hypointense signal at all concentrations greater than  $1 \times 10^5$  MSCs/1,000 mL on the back muscle of rats. Intracytoplasmic SPION were clearly visible at concentrations  $>1 \times 10^5$  SPION-MSCs (Fig. 2). *In vivo* MRI according to the duration of SPION-MSCs on the back muscle of rats showed a clear hypointense signal until 48 days after transplantation. SPION-MSCs injected into the corpus cavernosum of rats could be demonstrated by the distinct regional hypointense signal intensity induced by the susceptibility effects of the iron oxide particles (Fig. 3). The distribution of the hypointense signal intensity was located in the corpus cavernosa. On follow-up serial T2-weighted gradient-echo MRI, the hypointense signal intensity faded but persisted until 12 weeks after injection of SPION-labeled MSCs (Fig. 3).

## 4. Histological examination

The presence of iron oxide was also confirmed with Prussian blue staining 2 and 4 weeks after transplantation

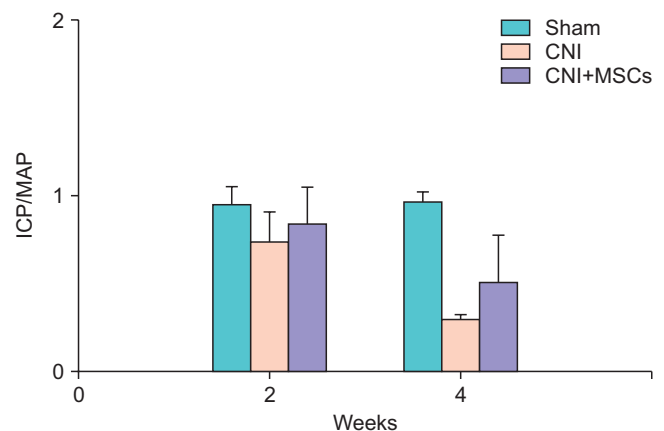


**Fig. 5.** Recovery of erection after 1-V electrical stimulation. ICP/MAP significantly decreased and recovered at 2 and 4 weeks after SPION-hMSCs transplantation. At 2 weeks after transplantation, sham vs. SPION-hMSCs noninjection,  $p < 0.05$ , sham vs. SPION-hMSCs injection,  $p < 0.05$ . At 4 weeks, after transplantation, sham vs. SPION-hMSCs noninjection,  $p < 0.05$ , sham vs. SPION-hMSCs injection,  $p < 0.05$ . Sham, sham operation; CNI, cavernous nerve injury; CNI+MSCs, mesenchymal stem cell transplantation after cavernous nerve injury; SPION, superparamagnetic iron oxide nanoparticles; hMSCs, human mesenchymal stem cells; ICP/MAP, ratio of maximal intracavernosal pressure to mean arterial pressure.

of SPION-labeled MSCs to rat corpus cavernosum (Fig. 4).

## 5. Recovery of erectile function after transplantation

The group with CN injury showed decreased ICP/MAP

( $0.76\pm 0.05$ ) at 2 weeks after CN injury ( $0.35\pm 0.09$ ,  $p<0.05$ ) compared with the sham group ( $0.76\pm 0.05$ ) and at 4 weeks after CN injury ( $0.25\pm 0.02$ ,  $p<0.05$ ) compared with the sham group ( $0.77\pm 0.04$ ) (Fig. 5). Transplantation of MSCs after CN injury was associated with increased ICP/MAP compared with that in the group with CN injury at 2 weeks ( $0.45\pm 0.13$ ,  $p<0.05$ ) and 4 weeks ( $0.41\pm 0.21$ ,  $p<0.05$ ) after CN injury (Fig. 5).

## DISCUSSION

In our previous report, we showed the multipotency of SPION-labeled human MSCs, which can be differentiated into osteogenic, chondrogenic, or adipogenic components by using Von Kossa, alkaline phosphatase, Toluidine blue, or Oil Red O staining, respectively [12-14]. Decreased signal intensity was also observed by *in vitro* MRI in the SPION-MSCs compared with distilled water and agarose gel without SPION-MSCs. To check the sensitivity of the MRI, we performed *in vitro* MRI with various concentrations of SPION-MSCs. A clear hypointense signal at all concentrations greater than  $1\times 10^5$  MSCs/1000  $\mu$ L was evident [12-14]. Building on our previous experience, we investigated the feasibility of *in vivo* monitoring of transplanted stem cells in the present study by using SPION labeling and MRI.

Various reports have illustrated the efficacy of stem cells in animal studies of ED [15-17]. In the present study, transplantation of MSCs after CN injury increased the ICP/MAP with electrical stimulation of 1 V compared with that in the group with CN injury at 2 and 4 weeks, which suggests that the MSCs recovered ED. After CN injury, the damage to penile cavernous smooth muscle cells and endothelial cells triggers collagen deposition [15] and heralds the development of ED. Because stem cell transplantation has the potential to restore normal function following injury, repair of cavernous smooth muscle cells and cavernous endothelial cells may be a novel means of treating ED.

MSCs are self-renewing stem cells with pluripotent capacity to differentiate into different cell types. For example, the potential differentiation of human MSCs transplanted in rat corpus cavernosum into endothelial or smooth muscle cells has been reported [13,14]. Inhibition of collagen deposition in rat bladder by transplantation of MSCs was also reported [12]. Improvement of ED after transplantation of MSCs appears to be associated with increased blood flow and decreased tissue hypoxia, which may contribute to improvement in histopathological and functional parameters [18]. Intracavernous application is a commonly used approach. In contrast with local injection of MSCs, intravenously administered MSCs are distributed

throughout the whole animal. Furthermore, there is concern about causing capillary clogging when larger cell types, such as MSCs, are infused, a complication that could result in hemodynamic compromise, interference with pulmonary gas exchange, and respiratory distress [19]. Intravenously injected MSCs are localized mainly to the pulmonary capillary bed [20]. Local injection may have a better effect than intravenous injection. MSCs are self-renewing adult stem cells with various differentiation potentials.

The relative ease of isolating MSCs from bone marrow and the great plasticity of the cells make them ideal tools for stem cell-based cell therapy. Recent studies have shown that *in vivo*, human MSCs transplanted into fetal sheep can differentiate into cells of various tissues [21], and transplanted cells show engraftment at ischemic lesions [16,17]. Also, animal experiments have shown that MSCs can prevent deleterious remodeling and improve recovery after myocardial infarction [22]. Therefore, MSCs fulfill all criteria of *in vivo* reconstitution of tissue [23].

The potential mechanism proposed for the therapeutic effects of MSCs is that MSCs are a source for cell replacement [24]. Transplanted human MSCs differentiate into endothelial or smooth muscle cells *in vivo* following engraftment in the corpus cavernosum. The present data implicate smooth muscle cells and endothelial cells in the improvement of ED in a rat model of CN injury. MSCs can secrete growth factors and contribute to reduced fibrosis through paracrine mechanisms rather than by cell incorporation [25,26]. MSCs may protect against injury by altering the microenvironment of the injury site at sites of engraftment. In a previous study, we showed that MSCs secrete many growth factors including nerve growth factor, brain-derived neurotrophic factor, neurotrophin-3, insulin-like growth factor, hepatocyte growth factor (HGF), glial cell line-derived neurotrophic factor, ciliary neurotrophic factor, and vascular endothelial growth factor [13]. Improvement of ED in the rat model of CN injury is due to enhanced regeneration of smooth muscle cells and endothelial cells by these growth factors. Collagen deposition in rats with bladder outlet obstruction can be inhibited by secreted HGF after transplantation of MSCs [12]. Improvement of ED in the rat model of CN injury is also due to decreased fibrosis of the corpus cavernosum.

Molecular imaging aims to visualize targeted cells in living organisms. Such cell trafficking studies would be a valuable tool for the development and evaluation of cell-based treatment strategies. To identify the migration of labeled cells by MRI, the contrast produced by the label must be sufficient to detect small clusters of cells and

simultaneously must not be toxic to the cell or the host. Cells labeled with SPION contrast that contains iron oxide particles exhibit much higher stability *in vivo* and reveal stronger contrast [27,28]. In this study, MSCs were separated and SPION were transferred to MSCs. Iron oxide-labeled cells appeared as hypointense areas in tissues associated with the decreased signal intensity on iron-sensitive T2-weighted and T2-weighted gradient echo images.

Due to their small crystal size, SPION exhibit magnetic moments that are unaffected by lattice orientation and align in an applied magnetic field. This alignment creates extremely large microscopic field gradients around the particles that de-phase the neighboring proton magnetic moments, thereby reducing the T2 relaxation time and facilitating the detection of labeled cells. Iron oxide particles are a Food and Drug Administration-approved MRI contrast agent. Thus, quality control, sterility, and stability have been well documented.

The use of transfection agents significantly improves the internalization of iron oxide particles without altering cell physiology and therefore is preferable for long-term MRI monitoring of labeled cells. SPION particles that are used for cellular labeling have not demonstrated any adverse effects in cell viability and differentiation of MSCs [10,27,29]. In this study, GenePORTER was not toxic to stem cell viability. Labeled MSCs also underwent normal chondrogenic, adipogenic, and osteogenic differentiation. Labeling stem cells with iron oxide particles enhances the cell-to-background contrast and makes them visible on MRI. *In vivo*, a decrease in MRI signal intensity was found in SPION-labeled MSCs by using GenePORTER, but not in other control groups including unlabeled MSCs. The intensity and area of the hypointense signal due to SPION depend on the concentration of iron oxide particles. *In vivo* experiments in the present study were performed to estimate the minimum concentration of iron oxide particles that would generate optimal contrast. Since the minimal concentration of  $1 \times 10^5$  SPION-labeled MSCs could be detected in the magnetic field, we believe that it will be possible to detect the cells if they form a cluster of  $1 \times 10^5$  or more. Thus, we decided to use a concentration of  $1 \times 10^6$  SPION-labeled MSCs in these studies.

In this study, we confirmed the ability of *in vivo* MRI to detect labeled stem cells in the corpus cavernosum of rats with CN injury. Serial imaging showed that the hypointense MRI signal was maintained for up to 4 weeks and then decreased over time. This could be due to dilution of iron after cell division or metabolism of iron oxide particles. The presence of MSCs in the corpus cavernosum of rats after

transplantation was confirmed with Prussian blue staining. Transplanted SPION-labeled MSCs were observed *in vivo* for up to 4 weeks and remained at or near the injection site.

## CONCLUSIONS

Transplanted SPION-labeled human MSCs were monitored by using MRI. SPION-labeled human MSCs transplanted into the corpus cavernosum of rats existed for up to 4 weeks after CN injury, and recovery of ED was evident. Our findings suggest that recovery of ED by use of SPION-labeled MSCs can be monitored *in vivo* by MRI.

## CONFLICTS OF INTEREST

The authors have nothing to disclose.

## ACKNOWLEDGMENTS

This research was supported by a Research Program through the National Research Foundation of Korea (NRF) funded by the Ministry of Education, Science and Technology (2010-0011678) and Soonchunhyang University Research Fund.

## REFERENCES

1. Quinlan DM, Epstein JI, Carter BS, Walsh PC. Sexual function following radical prostatectomy: influence of preservation of neurovascular bundles. *J Urol* 1991;145:998-1002.
2. Hatzimouratidis K, Burnett AL, Hatzichristou D, McCullough AR, Montorsi F, Mulhall JP. Phosphodiesterase type 5 inhibitors in postprostatectomy erectile dysfunction: a critical analysis of the basic science rationale and clinical application. *Eur Urol* 2009;55:334-47.
3. Montorsi F, Brock G, Lee J, Shapiro J, Van Poppel H, Graefen M, et al. Effect of nightly versus on-demand vardenafil on recovery of erectile function in men following bilateral nerve-sparing radical prostatectomy. *Eur Urol* 2008;54:924-31.
4. Fall PA, Izikki M, Tu L, Swieb S, Giuliano F, Bernabe J, et al. Apoptosis and effects of intracavernous bone marrow cell injection in a rat model of postprostatectomy erectile dysfunction. *Eur Urol* 2009;56:716-25.
5. Kendirci M, Trost L, Bakondi B, Whitney MJ, Hellstrom WJ, Spees JL. Transplantation of nonhematopoietic adult bone marrow stem/progenitor cells isolated by p75 nerve growth factor receptor into the penis rescues erectile function in a rat model of cavernous nerve injury. *J Urol* 2010;184:1560-6.
6. Ittrich H, Lange C, Dahnke H, Zander AR, Adam G, Nolte-

- Ernsting C. Labeling of mesenchymal stem cells with different superparamagnetic particles of iron oxide and detectability with MRI at 3T. *Rofo* 2005;177:1151-63.
7. Matuszewski L, Persigehl T, Wall A, Schwindt W, Tombach B, Fobker M, et al. Cell tagging with clinically approved iron oxides: feasibility and effect of lipofection, particle size, and surface coating on labeling efficiency. *Radiology* 2005;235:155-61.
  8. Bulte JW, Duncan ID, Frank JA. In vivo magnetic resonance tracking of magnetically labeled cells after transplantation. *J Cereb Blood Flow Metab* 2002;22:899-907.
  9. Song YS, Ku JH, Song ES, Kim JH, Jeon JS, Lee KH, et al. Magnetic resonance evaluation of human mesenchymal stem cells in corpus cavernosa of rats and rabbits. *Asian J Androl* 2007;9:361-7.
  10. Song YS, Ku JH. Monitoring transplanted human mesenchymal stem cells in rat and rabbit bladders using molecular magnetic resonance imaging. *Neurourol Urodyn* 2007;26:584-93.
  11. Pittenger MF, Mackay AM, Beck SC, Jaiswal RK, Douglas R, Mosca JD, et al. Multilineage potential of adult human mesenchymal stem cells. *Science* 1999;284:143-7.
  12. Lee HJ, Won JH, Doo SH, Kim JH, Song KY, Lee SJ, et al. Inhibition of collagen deposit in obstructed rat bladder outlet by transplantation of superparamagnetic iron oxide-labeled human mesenchymal stem cells as monitored by molecular magnetic resonance imaging (MRI). *Cell Transplant* 2012;21:959-70.
  13. Nagai A, Kim WK, Lee HJ, Jeong HS, Kim KS, Hong SH, et al. Multilineage potential of stable human mesenchymal stem cell line derived from fetal marrow. *PLoS One* 2007;2:e1272.
  14. Song YS, Lee HJ, Park IH, Kim WK, Ku JH, Kim SU. Potential differentiation of human mesenchymal stem cell transplanted in rat corpus cavernosum toward endothelial or smooth muscle cells. *Int J Impot Res* 2007;19:378-85.
  15. Iacono F, Giannella R, Somma P, Manno G, Fusco F, Mirone V. Histological alterations in cavernous tissue after radical prostatectomy. *J Urol* 2005;173:1673-6.
  16. Kalka C, Masuda H, Takahashi T, Kalka-Moll WM, Silver M, Kearney M, et al. Transplantation of ex vivo expanded endothelial progenitor cells for therapeutic neovascularization. *Proc Natl Acad Sci U S A* 2000;97:3422-7.
  17. Orlic D, Kajstura J, Chimenti S, Jakoniuk I, Anderson SM, Li B, et al. Bone marrow cells regenerate infarcted myocardium. *Nature* 2001;410:701-5.
  18. Woo LL, Tanaka ST, Anumanthan G, Pope JC 4th, Thomas JC, Adams MC, et al. Mesenchymal stem cell recruitment and improved bladder function after bladder outlet obstruction: preliminary data. *J Urol* 2011;185:1132-8.
  19. Gao J, Dennis JE, Muzic RF, Lundberg M, Caplan AI. The dynamic in vivo distribution of bone marrow-derived mesenchymal stem cells after infusion. *Cells Tissues Organs* 2001;169:12-20.
  20. Schrepfer S, Deuse T, Reichenspurner H, Fischbein MP, Robbins RC, Pelletier MP. Stem cell transplantation: the lung barrier. *Transplant Proc* 2007;39:573-6.
  21. Liechty KW, MacKenzie TC, Shaaban AF, Radu A, Moseley AM, Deans R, et al. Human mesenchymal stem cells engraft and demonstrate site-specific differentiation after in utero transplantation in sheep. *Nat Med* 2000;6:1282-6.
  22. Pittenger MF, Martin BJ. Mesenchymal stem cells and their potential as cardiac therapeutics. *Circ Res* 2004;95:9-20.
  23. Verfaillie CM. Adult stem cells: assessing the case for pluripotency. *Trends Cell Biol* 2002;12:502-8.
  24. Sharma AD, Cantz T, Manns MP, Ott M. The role of stem cells in physiology, pathophysiology, and therapy of the liver. *Stem Cell Rev* 2006;2:51-8.
  25. Kinnaird T, Stabile E, Burnett MS, Shou M, Lee CW, Barr S, et al. Local delivery of marrow-derived stromal cells augments collateral perfusion through paracrine mechanisms. *Circulation* 2004;109:1543-9.
  26. Silva GV, Litovsky S, Assad JA, Sousa AL, Martin BJ, Vela D, et al. Mesenchymal stem cells differentiate into an endothelial phenotype, enhance vascular density, and improve heart function in a canine chronic ischemia model. *Circulation* 2005;111:150-6.
  27. Bulte JW, Douglas T, Witwer B, Zhang SC, Strable E, Lewis BK, et al. Magnetodendrimers allow endosomal magnetic labeling and in vivo tracking of stem cells. *Nat Biotechnol* 2001;19:1141-7.
  28. Kraitchman DL, Heldman AW, Atalar E, Amado LC, Martin BJ, Pittenger MF, et al. In vivo magnetic resonance imaging of mesenchymal stem cells in myocardial infarction. *Circulation* 2003;107:2290-3.
  29. Kostura L, Kraitchman DL, Mackay AM, Pittenger MF, Bulte JW. Feridex labeling of mesenchymal stem cells inhibits chondrogenesis but not adipogenesis or osteogenesis. *NMR Biomed* 2004;17:513-7.